J. Fluid Mech. (1983), *vol.* 132, *pp.* 431–444
Printed in Great Britain

Practical use of Hamilton's principle

By RICK SALMON
Scripps Institution of Oceanography, La Jolla, CA 92093

(Received 17 December 1982 and in revised form 4 March 1983)

Hamilton's principle of mechanics has special advantages as the beginning point for approximations. First, it is extremely succinct. Secondly, it easily accommodates moving disconnecting fluid boundaries. Thirdly, approximations – however strong – that maintain the symmetries of the Hamiltonian will automatically preserve the corresponding conservation laws. For example, Hamilton's principle allows useful analytical and numerical approximations to the equations governing the motion of a homogeneous rotating fluid with free boundaries.

1. Introduction

Hamilton's principle of mechanics governs the motions of classical fluids. As a statement of dynamical law, it has important practical advantages over the more conventional Eulerian formulation of fluid mechanics. In this paper, I show how Hamilton's principle permits useful analytical and numerical approximations to the equations governing the motion of a homogeneous fluid blob on an infinite rotating table (figure 1). The blob is horizontally unconstrained, and can subdivide into any number of 'bloblets'. Salmon (1982*a*) used a similar model system for a numerical study of the ocean's main thermocline. In this paper, the blob model serves merely to illustrate the special advantages of Hamiltonian methods, which generalize easily to more complicated cases. The methods described below are distinctly superior to those of the earlier paper.

Hamilton's principle has two primary advantages as the beginning point for approximations. First, it is extremely succinct. This means, for example, that, once the exact Hamiltonian has been replaced by a discrete numerical analogue, then the numerical analyst is relieved of all further opportunities to exercise his bias: the principle of least action dictates the evolution equations for the discrete dependent variables. Secondly, there exists a well-known connection between the symmetry properties of the Hamiltonian and the conservation laws of the dynamical system. Approximations – however strong – that maintain the symmetries will automatically preserve analogues of the exact constants of the motion.

Hamilton's principle for perfect fluids can be stated in a great many dissimilar forms, which differ in the choice of both dependent and independent variables. The commonly encountered forms of Hamilton's principle fall into two general categories. In the first category, which corresponds to Hamilton's principle in particle mechanics, the positions and momenta of marked fluid particles are varied at fixed times (Herivel 1955; Eckart 1960). This is the form of Hamilton's principle used in this paper. In the second category, appropriately chosen field variables are varied at fixed locations and times. The field variables typically include a set of scalar potentials which represent the fluid velocity (Clebsch 1859; Seliger & Whitham 1968). It has recently been shown that these two general forms of Hamilton's principle are really the same: They are related by canonical transformations (Broer & Kobussen 1974; van Saarloos

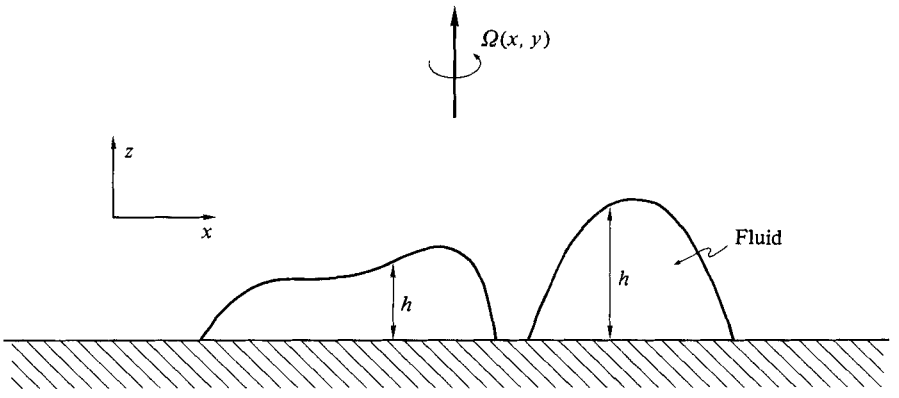

FIGURE 1. The general fluid system considered in this paper.

1981; Salmon 1982*a*; Griffa 1982). I believe that the particle form is usually the simplest, and that the others have been somewhat overemphasized.

This paper is self-contained and requires only an elementary familiarity with Hamiltonian mechanics. Section 2 defines the blob model, with 'shallow-water' dynamics, gives the equivalent form of Hamilton's principle, and derives the important conservation laws. The numerical model of §3 is an energy-conserving analogue which easily accommodates blob splitting and reconnection. In contrast with the awkward method of Salmon (1982*a*), the fluid particles need never be relabelled. However, because the model of §§2 and 3 includes fast gravity waves, it is inefficient for the study of low-frequency motions. Section 4 therefore introduces an approximate Hamiltonian in which the momenta are replaced *a priori* by their geostrophic values. The resulting equations, which contain no gravity waves, resemble 'balanced models' currently in use. However, these new equations conserve proper analogues of the total energy and the potential vorticity on fluid particles. Section 5 applies the numerical model of §3 to an example of current interest.

Hamilton's principle has not often been used as the basis for numerical models. The point vortex model of incompressible two-dimensional flow is a notable exception (see e.g. Aref & Pomphrey 1981). Buneman (1982) describes a two-dimensional model based upon the Clebsch formulation of Hamilton's principle. His method will require particle relabelling (a gauge transformation of the Clebsch potentials) to maintain numerical accuracy as time increases. The best known numerical models for flows with free surfaces and arbitrary vorticity distributions are the marker- and particle-in-cell methods, which are not based upon a Hamiltonian (see e.g. Harlow & Welch 1965).

2. Shallow-water model

The equations governing a shallow rotating blob of inviscid homogeneous fluid are

$$\frac{\mathrm{D}u}{\mathrm{D}t} - fv = -g\frac{\partial h}{\partial x}, \tag{2.1a}$$

$$\frac{\mathrm{D}v}{\mathrm{D}t} + fu = -g\frac{\partial h}{\partial y}, \tag{2.1b}$$

$$\frac{\partial h}{\partial t} + \frac{\partial}{\partial x}(uh) + \frac{\partial}{\partial y}(vh) = 0, \tag{2.1c}$$

where (x, y) are the horizontal Cartesian coordinates, (u, v) the corresponding horizontal velocities, t is the time, $\mathrm{D}/\mathrm{D}t = \partial/\partial t + u\,\partial/\partial x + v\,\partial/\partial y$, $f = 2\Omega$ is the Coriolis parameter, $\Omega(x, y)$ is the spatially variable rotation rate, g is gravity, and $h(x, y, t)$ is the depth of the fluid (see figure 1).

Equations (2.1) are valid when the lengthscale L for horizontal variability is large compared with the fluid depth H, i.e.

$$\left(\frac{H}{L}\right)^2 \ll 1. \tag{2.2}$$

Then the pressure is hydrostatic and the horizontal velocity depth-independent. The same applies to flow in rapidly rotating coordinates under the weaker condition

$$\frac{U}{\Omega L}\left(\frac{H}{L}\right)^2 \ll 1, \tag{2.3}$$

where U is the scale for horizontal velocity.

Before introducing the form of Hamilton's principle corresponding to (2.1), it is appropriate to review basic particle mechanics. Consider therefore a classical system composed of N discrete particles. Let i be a subscript index which identifies the particle and let m_i and $\boldsymbol{x}_i(\tau)$ be the mass and the Cartesian position of the ith particle at time τ. Let $V(\boldsymbol{x}_1, \ldots, \boldsymbol{x}_N)$ be the potential energy of the system. The Lagrangian is

$$L = \left(\sum_{i=1}^{N} \tfrac{1}{2} m_i \dot{\boldsymbol{x}}_i \cdot \dot{\boldsymbol{x}}_i\right) - V(\boldsymbol{x}_1, \ldots, \boldsymbol{x}_N), \tag{2.4}$$

and the dynamical equations result from Hamilton's principle in the form

$$\delta \int_{-\infty}^{-\infty} L \,\mathrm{d}\tau = 0, \tag{2.5}$$

where δ corresponds to arbitrary variations $\delta\boldsymbol{x}_i(\tau)$ in the particle trajectories, and $\delta\boldsymbol{x}_i(\pm\infty) = 0$. Alternatively, one can define the conjugate momenta

$$\boldsymbol{p}_i \equiv \frac{\partial L}{\partial \dot{\boldsymbol{x}}_i}, \tag{2.6}$$

and invoke Hamilton's principle in the 'extended form'

$$\delta \int \mathrm{d}\tau \left\{\sum_i \boldsymbol{p}_i \cdot \dot{\boldsymbol{x}}_i - H(\boldsymbol{x}_1, \boldsymbol{p}_1, \ldots, \boldsymbol{x}_N, \boldsymbol{p}_N)\right\} = 0, \tag{2.7}$$

where

$$H = \sum_i \boldsymbol{p}_i \cdot \dot{\boldsymbol{x}}_i - L \tag{2.8}$$

is the Hamiltonian and δ now stands for arbitrary independent variations $\delta\boldsymbol{p}_i(\tau)$, $\delta\boldsymbol{x}_i(\tau)$ in the momenta and positions of the particles.

Now consider the blob. Suppose first that $f = 0$. Let the positions

$$x = x(a, b, \tau), \quad y = y(a, b, \tau) \tag{2.9}$$

of marked fluid particles be considered as functions of curvilinear labelling coordinates (a, b) and the time τ. The labelling coordinates remain constant following the columnar motion of the fluid particles, and they are analogous to the subscript i above. Note that $\tau = t$, but $\partial/\partial t$ means that (x, y) are held fixed, while $\partial/\partial\tau$ means fixed

(a, b). Thus $\partial/\partial\tau \equiv \mathrm{D}/\mathrm{D}t$. It is convenient to assign the labelling coordinates so that equal areas in (a, b)-space contain equal masses. Then

$$\mathrm{d(mass)} = \mathrm{d}a\,\mathrm{d}b = \rho h\,\mathrm{d}x\,\mathrm{d}y,$$

$$h = \frac{1}{\rho}\frac{\partial(a,b)}{\partial(x,y)}, \tag{2.10}$$

where ρ is the constant fluid density. Apply $\partial/\partial\tau$ to (2.10). The result is (2.1c). Thus mass conservation is implicit in the representation (2.9).

The blob kinetic energy (omitting the contribution of the vertical velocity) is

$$T = \frac{1}{2}\int\int \mathrm{d}a\,\mathrm{d}b\,\frac{\partial \boldsymbol{x}}{\partial\tau}\cdot\frac{\partial \boldsymbol{x}}{\partial\tau}, \tag{2.11}$$

where the integration runs over the entire area of the blob. The potential energy is

$$V = \tfrac{1}{2}g\int\int \mathrm{d}a\,\mathrm{d}b\,h. \tag{2.12}$$

In (2.12) and below, the symbol h should be considered an abbreviation for the right-hand side of (2.10). Let

$$L = T - V,$$

and require

$$\delta\int L\,\mathrm{d}\tau = 0$$

for arbitrary variations $\delta x(a, b, \tau)$, $\delta y(a, b, \tau)$. The methods of variational calculus yield

$$\delta x\colon\ \delta\int L\,\mathrm{d}\tau = \int \mathrm{d}\tau\int\int \mathrm{d}a\,\mathrm{d}b\left[\frac{\partial x}{\partial\tau}\frac{\partial\delta x}{\partial\tau} + \frac{\rho g}{2}h^2\frac{\partial(\delta x, y)}{\partial(a,b)}\right]$$

$$= \int\int\int \mathrm{d}\tau\,\mathrm{d}a\,\mathrm{d}b\left[-\frac{\partial^2 x}{\partial\tau^2} - \frac{\rho g}{2}\frac{\partial(h^2, y)}{\partial(a,b)}\right]\delta x. \tag{2.13}$$

The last step uses $h = 0$ at blob boundaries. Since δx is arbitrary, (2.13) implies that

$$\frac{\partial^2 x}{\partial\tau^2} = -\rho g h\frac{\partial(x,y)}{\partial(a,b)}\frac{\partial(h,y)}{\partial(x,y)} = -g\frac{\partial h}{\partial x}, \tag{2.14}$$

which is equivalent to (2.1a) when $f = 0$. Similarly, of course,

$$\delta y\colon\ \frac{\partial^2 y}{\partial\tau^2} = -g\frac{\partial h}{\partial y}. \tag{2.15}$$

To derive the extended form of Hamilton's principle for the blob, define

$$u \equiv \frac{\delta L}{\delta(\partial x/\partial\tau)}, \quad v \equiv \frac{\delta L}{\delta(\partial y/\partial\tau)}$$

where δ denotes the functional derivative. The analogues of (2.7), (2.8) are

$$\delta\int \mathrm{d}\tau\left\{\int\int \mathrm{d}a\,\mathrm{d}b\,u\frac{\partial x}{\partial\tau} + v\frac{\partial y}{\partial\tau} - H\right\} = 0, \tag{2.16}$$

$$H = \frac{1}{2}\int\int \mathrm{d}a\,\mathrm{d}b\,[u^2 + v^2 + gh]. \tag{2.17}$$

Independent variations δx, δy, δu, $\delta v(a, b, \tau)$ now yield (2.14), (2.15) plus

$$u = \frac{\partial x}{\partial\tau}, \quad v = \frac{\partial y}{\partial\tau}. \tag{2.18}$$

Next suppose that f is a non-zero constant. The principle (2.16) still holds in the coordinate system fixed to the stars. An elementary transformation to rotating coordinates gives the Lagrangian

$$L = \int\int da\, db \left[(u - \Omega y)\frac{\partial x}{\partial \tau} + (v + \Omega x)\frac{\partial y}{\partial \tau} - \frac{\Omega^2}{2} x \cdot x \right] - H. \tag{2.19}$$

The Ω^2 term in (2.19) induces centrifugal acceleration, which was neglected in (2.1).† If this term is dropped from (2.19), then the variational equations are just (2.1). Finally, for the case of non-constant rotation, the proper generalization of (2.19) is

$$L = \int\int da\, db \left[(u - R)\frac{\partial x}{\partial \tau} + (v + P)\frac{\partial y}{\partial \tau} \right] - H, \tag{2.20}$$

where $R(x, y)$ and $P(x, y)$ are any two functions satisfying

$$\frac{\partial R}{\partial y} + \frac{\partial P}{\partial x} = f(x, y). \tag{2.21}$$

The Lagrangian (2.20) is precisely equivalent to the dynamics (2.1) for general $f(x, y)$.

The conservation laws for (2.1) can be deduced from the symmetry properties of (2.20). This procedure will seem roundabout, but the reader should reserve his judgement until §4. The conservation of energy corresponds to the symmetry property that R, P and g contain no explicit time dependence. Let

$$\tau' = \tau + \delta\tau(\tau), \quad \delta\tau \to 0, \quad \delta\tau(\pm\infty) = 0 \tag{2.22}$$

be a new time coordinate and let the dependence of x, y, u, v on τ in one realization of the motion be the same as the dependence on τ' in a second realization. The two realizations differ only in the time values assigned to corresponding events. The action difference between the two realizations is

$$\begin{aligned}
&\int d\tau' L\left[x, y, u, v, \frac{\partial x}{\partial \tau'}, \frac{\partial y}{\partial \tau'}\right] - \int d\tau L\left[x, y, u, v, \frac{\partial x}{\partial \tau}, \frac{\partial y}{\partial \tau}\right] \\
&= \int d\tau \frac{d\tau'}{d\tau} L\left[x, y, u, v, \frac{\partial x}{\partial \tau}\frac{d\tau}{d\tau'}, \frac{\partial y}{\partial \tau}\frac{d\tau}{d\tau'}\right] - \int d\tau L \\
&= \int d\tau \left(\frac{d\delta\tau}{d\tau}\right)\left[L - \int\int da\, db \frac{\delta L}{\delta(\partial x/\partial \tau)}\frac{\partial x}{\partial \tau} + \frac{\delta L}{\delta(\partial y/\partial \tau)}\frac{\partial y}{\partial \tau}\right] + O(\delta\tau^2) \\
&= \int d\tau \left(\frac{d\delta\tau}{d\tau}\right) H + O(\delta\tau^2) \\
&= -\int d\tau\, \delta\tau \frac{dH}{d\tau} + O(\delta\tau^2),
\end{aligned} \tag{2.23}$$

which must be zero by Hamilton's principle. Thus

$$\frac{dH}{d\tau} = 0. \tag{2.24}$$

† More precisely, the centrifugal accelerations were considered to be a part of the gravity, which was still treated as locally Cartesian.

Potential-vorticity conservation corresponds to the symmetry property that the labelling coordinates (a, b) enter (2.20) only through the Jacobian (2.10). Let

$$\left.\begin{aligned} a' &= a+\delta a(a,b,\tau), \\ b' &= b+\delta b(a,b,\tau) \end{aligned}\right\} \tag{2.25}$$

be new labelling coordinates with the same value of (2.10). Now, δ corresponds to changes in the values of the particle labels only. That is, the two realizations differ only in the label values assigned to corresponding particles. By assumption,

$$\begin{aligned} 0 &= \delta\frac{\partial(a,b)}{\partial(x,y)} \\ &= \frac{\partial(a,b)}{\partial(x,y)}\left[\frac{\partial\delta a}{\partial a}+\frac{\partial\delta b}{\partial b}\right] \end{aligned} \tag{2.26}$$

implies that

$$\delta a = -\frac{\partial\delta\psi}{\partial b}, \quad \delta b = +\frac{\partial\delta\psi}{\partial a} \tag{2.27}$$

for some $\delta\psi(a,b,\tau)$. The change in action is

$$\delta\int L\,\mathrm{d}\tau = \int\mathrm{d}\tau\iint\mathrm{d}a\,\mathrm{d}b\left[(u-R)\,\delta\frac{\partial x}{\partial\tau}+(v+P)\,\delta\frac{\partial y}{\partial\tau}\right], \tag{2.28}$$

where

$$\begin{aligned} \delta\frac{\partial x}{\partial\tau} &= \left.\frac{\partial x}{\partial\tau}\right|_{a',\,b'} - \left.\frac{\partial x}{\partial\tau}\right|_{a,\,b} \\ &= -\frac{\partial x}{\partial a}\frac{\partial\delta a}{\partial\tau}-\frac{\partial x}{\partial b}\frac{\partial\delta b}{\partial\tau}, \end{aligned} \tag{2.29}$$

and similarly

$$\delta\frac{\partial y}{\partial\tau} = -\frac{\partial y}{\partial a}\frac{\partial\delta a}{\partial\tau}-\frac{\partial y}{\partial b}\frac{\partial\delta b}{\partial\tau}. \tag{2.30}$$

Thus

$$\begin{aligned} \delta\int L\,\mathrm{d}\tau &= -\int\mathrm{d}\tau\iint\mathrm{d}a\,\mathrm{d}b\left\{\delta a\frac{\partial}{\partial\tau}\left[(u-R)\frac{\partial x}{\partial a}+(v+P)\frac{\partial y}{\partial a}\right]\right. \\ &\qquad \left.+\delta b\frac{\partial}{\partial\tau}\left[(u-R)\frac{\partial x}{\partial b}+(v+P)\frac{\partial y}{\partial b}\right]\right\} \\ &= \int\mathrm{d}\tau\iint\mathrm{d}a\,\mathrm{d}b\,\delta\psi\frac{\partial}{\partial\tau}\left[\frac{\partial(u-R,x)}{\partial(a,b)}+\frac{\partial(v+P,y)}{\partial(a,b)}\right] \\ &= \rho\int\mathrm{d}\tau\iint\mathrm{d}a\,\mathrm{d}b\,\delta\psi\frac{\partial}{\partial\tau}\left[\left(\frac{\partial v}{\partial x}-\frac{\partial u}{\partial y}+f\right)\frac{1}{h}\right]. \end{aligned} \tag{2.31}$$

Since $\delta\psi$ is arbitrary,

$$\frac{\partial}{\partial\tau}\left[\left(\frac{\partial v}{\partial x}-\frac{\partial u}{\partial y}+f\right)\frac{1}{h}\right] = 0, \tag{2.32}$$

and the potential vorticity is conserved on particles. This derivation has been given in a more general form by Ripa (1981) and Salmon (1982*b*).

Although energy and potential vorticity seem to be the most important invariants, there may of course be others. Momentum and angular-momentum conservation correspond to translational and rotational invariance of the whole system. Solid boundaries (and other external potentials) affect the conservation of momentum but not the potential vorticity, because the latter depends only on particle-label variations.

3. Numerical analogue

Suppose that the continuous blob is replaced by a collection of N discrete particles, each with mass m. Let $\boldsymbol{x}_i$ be the (x, y)-location of the ith particle. According to (2.10) ths fluid depth is proportional to the mass per unit area. This motivates the replacement

$$h(\boldsymbol{x}) = \frac{m}{\rho} n(\boldsymbol{x}), \tag{3.1}$$

where

$$n(\boldsymbol{x}) = \iint \mathrm{d}\boldsymbol{x}_0 \, S(|\boldsymbol{x}-\boldsymbol{x}_0|) \sum_{i=1}^{N} \delta(\boldsymbol{x}_0-\boldsymbol{x}_i)$$

$$= \sum_i S(|\boldsymbol{x}_i-\boldsymbol{x}|) \tag{3.2}$$

is a smooth estimator of the number of particles per unit area. The 'sampling function' $S(r)$ is a bell-shaped function of radius r_0 centred on $r = 0$. Since

$$N = \iint \mathrm{d}\boldsymbol{x} \, n(\boldsymbol{x}),$$

the function $S(r)$ must satisfy

$$2\pi \int_0^{r_0} rS(r) \, \mathrm{d}r = 1. \tag{3.3}$$

The specific choice

$$S(r) = \begin{cases} \dfrac{10}{3\pi r_0^2}\left[1-3\left(\dfrac{r}{r_0}\right)^2+2\left(\dfrac{r}{r_0}\right)^3\right] & (r \leqslant r_0), \\ 0 \quad (r > r_0) \end{cases} \tag{3.4}$$

satisfies (3.3) and

$$S'(0) = S'(r_0) = S(r_0) = 0. \tag{3.5}$$

The parameter r_0 controls spatial resolution. If r_0 is too large, then the resolving power of (3.2) is poor. However, if r_0 is too small for the number of particles present, then the estimator $n(\boldsymbol{x})$ has 'lumps' at the locations of the particles. The calculation is insensitive to the precise form of $S(r)$ provided that the particle concentration is sufficiently great.

Now replace the Lagrangian (2.20) by the discrete analogue,

$$L = \sum_i m\left[(u_i-R_i)\,\dot{x}_i+(v_i+P_i)\,\dot{y}_i-\frac{1}{2}\left(u_i^2+v_i^2+\frac{mg}{\rho}n(\boldsymbol{x}_i)\right)\right], \tag{3.6}$$

where (u_i, v_i) is the velocity of the ith particle and

$$R_i = R(\boldsymbol{x}_i), \quad P_i = P(\boldsymbol{x}_i). \tag{3.7}$$

The numerical dynamics come from Hamilton's principle in the form

$$\delta \int L \, \mathrm{d}\tau = 0,$$

where L is given by (3.6) and δ now corresponds to arbitrary independent variations $\delta x_i(\tau)$, $\delta y_i(\tau)$, $\delta u_i(\tau)$, $\delta v_i(\tau)$. The variational equations are

$$\delta u_i\colon \ \dot{x}_i = u_i, \tag{3.8a}$$

$$\delta v_i\colon \ \dot{y}_i = v_i, \tag{3.8b}$$

$$\delta x_i\colon\ \dot{u}_i - f_i v_i = -\frac{gm}{\rho}\sum_j \frac{\partial S}{\partial x_i}(|\boldsymbol{x}_i - \boldsymbol{x}_j|), \tag{3.8c}$$

$$\delta y_i\colon\ \dot{v}_i + f_i u_i = -\frac{gm}{\rho}\sum_j \frac{\partial S}{\partial y_i}(|\boldsymbol{x}_i - \boldsymbol{x}_j|), \tag{3.8d}$$

where $$f_i = f(x_i, y_i).$$

Equations (3.8) are a coupled set of ordinary differential equations in the variables $\{x_i, y_i, u_i, v_i\}$. They can easily be solved by standard numerical methods. The analogues of (2.1 a, b) are (3.8 c, d). As in the continuous case, the conservation of mass (2.1 c) is implicit in the particle representation. The dynamics (3.8) automatically conserve the discrete energy

$$H = \tfrac{1}{2}m\sum_i (u_i^2 + v_i^2) + \frac{m^2 g}{2\rho}\sum_i\sum_j S(|\boldsymbol{x}_i - \boldsymbol{x}_j|). \tag{3.9}$$

The sampling function $S(r)$ enters (3.8), (3.9) as the potential for a repulsive force between particles. This potential is finite for zero particle separation and zero for separations greater than r_0. Thus the right-hand sides of (3.8), (3.9) demand only $O(N)$ computations, which is the same as for standard gridpoint methods. However, unlike gridpoint methods, (3.8) easily accommodates moving and disconnecting blob boundaries. The boundary particles have no special status in (3.8).

From the standpoint of oceanographic applications (3.8) have two shortcomings. First, there is apparently no discrete analogue of the potential-vorticity conservation on particles. I will return to this point in §6. Secondly, and more important, the dynamics (3.8) correctly include gravity waves. These waves, which all have frequencies greater than f, are a great hindrance to the efficient numerical study of low-frequency motion, because the gravity waves require a very short time step for numerical stability. Section 4 offers a low-frequency approximation to (3.6) which filters out the gravity waves but retains the other advantages of (3.8).

4. Geostrophic model

Suppose that the velocity variables (u, v) are simply dropped from (2.20). The resulting Lagrangian,

$$L_0 = \int\int da\, db\left[-R\frac{\partial x}{\partial \tau} + P\frac{\partial y}{\partial \tau} - \frac{g}{2\rho}\frac{\partial(a,b)}{\partial(x,y)}\right], \tag{4.1}$$

depends only on the particle locations $\boldsymbol{x}(a, b, \tau)$. Variations in the particle locations yield

$$\delta x\colon\ -f\frac{\partial y}{\partial \tau} = -g\frac{\partial h}{\partial x}, \tag{4.2a}$$

$$\delta y\colon\ +f\frac{\partial x}{\partial \tau} = -g\frac{\partial h}{\partial y}, \tag{4.2b}$$

which are the equations of geostrophic balance. Since mass conservation is still implicit, these dynamics are equivalent to the following set of Eulerian equations:

$$-fv = -g\frac{\partial h}{\partial x}, \quad +fu = -g\frac{\partial h}{\partial y}, \tag{4.3a,b}$$

$$\frac{\partial h}{\partial t} + \frac{\partial}{\partial x}(uh) + \frac{\partial}{\partial y}(vh) = 0 \tag{4.3c}$$

for the dependent variables u, v and $h(x, y, t)$. The set (4.3) is a logical approximation to low-Rossby-number flow ($U/\Omega L \ll 1$). However, the complete neglect of inertia is probably too severe. If, for example, f is constant, then the Eulerian motion described by (4.3) is steady, and the particles follow periodic orbits.

Suppose therefore that (u, v) are not dropped, but replaced *a priori* by their geostrophic values. The resulting Lagrangian

$$L_1 = \int\int da\, db \left[(u_G - R)\frac{\partial x}{\partial \tau} + (v_G + P)\frac{\partial y}{\partial \tau} - \tfrac{1}{2}(u_G^2 + v_G^2 + gh) \right], \tag{4.4}$$

with

$$u_G \equiv -\frac{g}{f}\frac{\partial h}{\partial y}, \quad v_G \equiv +\frac{g}{f}\frac{\partial h}{\partial x}, \tag{4.5}$$

still depends only on the particle locations, because the geostrophic velocities are determined by the mass distribution. Variations in the particle locations now yield

$$h\left[\frac{\partial}{\partial t}\boldsymbol{u}_G + \boldsymbol{u}_G \cdot \nabla \boldsymbol{u}_G + \boldsymbol{u}_G \cdot \nabla \boldsymbol{u}_{AG} + \boldsymbol{u}_{AG} \cdot \nabla \boldsymbol{u}_G\right] + f\hat{\boldsymbol{k}} \times h(\boldsymbol{u}_G + \boldsymbol{u}_{AG}) + g\nabla(\tfrac{1}{2}h^2)$$

$$= -g\nabla\left(h^2 \hat{\boldsymbol{k}} \cdot \nabla \times \left(\frac{\boldsymbol{u}_{AG}}{f}\right)\right) - g\nabla(\tfrac{1}{2}h^2)\left[\boldsymbol{u}_{AG} \times \nabla\left(\frac{1}{f}\right)\right] \cdot \hat{\boldsymbol{k}}, \tag{4.6}$$

where the ageostrophic velocity

$$\boldsymbol{u}_{AG} \equiv \frac{\partial \boldsymbol{x}}{\partial \tau} - \boldsymbol{u}_G \tag{4.7}$$

is the difference between the 'true velocity' $\partial \boldsymbol{x}/\partial \tau$ of massive particles, and the geostrophic velocity $\boldsymbol{u}_G$. From the Lagrangian viewpoint, (4.6) is a first-order equation in time for the particle locations $\boldsymbol{x}(a, b, \tau)$. The symbols $\boldsymbol{u}_G$ and $\boldsymbol{u}_{AG}$ are merely abbreviations for (4.5) and (4.7). From the Eulerian point of view, (4.5), (4.6) and the continuity equation

$$\frac{\partial h}{\partial t} + \nabla \cdot [(\boldsymbol{u}_G + \boldsymbol{u}_{AG})h] = 0 \tag{4.8}$$

are five equations in the five dependent variables $\boldsymbol{u}_G$, $\boldsymbol{u}_{AG}$, and $h(x, y, t)$. There is no explicit equation for the time evolution of $\boldsymbol{u}_{AG}$, but an equation determining $\boldsymbol{u}_{AG}$ from h could be obtained by time differentiation of (4.5) and the use of (4.6) and (4.8). The Lagrangian viewpoint is much simpler, and is the form preferred for numerical study. However, the Eulerian form (4.6) reveals some of the physical content of (4.4). The left side of (4.6) contains the exact Coriolis and pressure-gradient terms, plus an approximation

$$\frac{\partial}{\partial t}\boldsymbol{u}_G + \boldsymbol{u}_G \cdot \nabla \boldsymbol{u}_G + \boldsymbol{u}_G \cdot \nabla \boldsymbol{u}_{AG} + \boldsymbol{u}_{AG} \cdot \nabla \boldsymbol{u}_G \tag{4.9}$$

to the exact relative acceleration

$$\frac{\partial}{\partial \tau}(\boldsymbol{u}_G + \boldsymbol{u}_{AG}). \tag{4.10}$$

The approximation (4.9) differs from (4.10) in the neglect of the local rate of change in the ageostrophic velocity, $\partial \boldsymbol{u}_{AG}/\partial t$ and in the neglect of $\boldsymbol{u}_{AG} \cdot \nabla \boldsymbol{u}_{AG}$. Both terms are small in low-Rossby-number flow. The neglect of $\partial \boldsymbol{u}_{AG}/\partial t$ filters out the gravity waves. The right-hand side of (4.6) has no obvious interpretation, but is no larger than the smallest terms on the left, provided that the scale for f variation is no smaller than L. For constant f, the right-hand side of (4.6) reduces to

$$-g\nabla\left(h^2 \frac{\zeta_{AG}}{f}\right), \tag{4.11}$$

where ζ_{AG} is the ageostrophic relative vorticity. The expression (4.11) can be considered as a tiny error in the pressure gradient.

The conservation laws for (4.6) follow directly from the symmetry properties of (4.4). The dynamics (4.4) or (4.6) conserves the 'geostrophic energy',

$$\frac{\mathrm{d}}{\mathrm{d}t}\frac{1}{2}\int\int \mathrm{d}a\,\mathrm{d}b\,(u_G^2+v_G^2+gh)=0, \tag{4.12}$$

and a geostrophic approximation to the potential vorticity on particles,

$$\frac{\partial}{\partial\tau}\left[\left(\frac{\partial v_G}{\partial x}-\frac{\partial u_G}{\partial y}+f\right)\frac{1}{h}\right]=0. \tag{4.13}$$

These laws are easily proved using the same methods as in §2. Again, the potential-vorticity law (4.13) results from variations in the particle labels which leave the Jacobian (2.10) unchanged. These conservation laws can of course also be proved directly from (4.6), but the algebra is surprisingly tedious. More important, the appearance of (4.6) gives no hint that conservation laws even exist, whereas the obvious symmetry properties of (4.4) guarantee *a priori* that analogues of the energy and potential vorticity will be conserved. From the Eulerian viewpoint, the peculiar terms on the right-hand side of (4.6) are, miraculously, just those required to get (4.12) and (4.13). From the Lagrangian viewpoint (4.12), (4.13) are secure from the beginning. In a sense, (4.12), (4.13) are more important than the appearance of (4.6), because the *existence* of conservation laws and symmetry properties is independent of the choice of coordinates. That the approximation (4.4) leads to complicated Eulerian equations is not a deficiency in the approximation itself, but rather in the choice of an Eulerian representation.

The discrete analogue of (4.4) is

$$L_1=\sum_i m[(u_{Gi}-R_i)\,\dot{x}_i+(v_{Gi}+P_i)\,\dot{y}_i-\tfrac{1}{2}(u_{Gi}^2+v_{Gi}^2+gh_i)], \tag{4.14}$$

where

$$(u_G,v_G)_i=\frac{g}{f_i}\left(-\frac{\partial h_i}{\partial y_i},\frac{\partial h_i}{\partial x_i}\right), \tag{4.15}$$

$$h_i=h(\boldsymbol{x}_i)=\frac{m}{\rho}\sum_j S(|\boldsymbol{x}_i-\boldsymbol{x}_j|) \tag{4.16}$$

as before. The discrete dynamics

$$-q_i\,\dot{y}_i=\sum_{j\neq i}\left[\left(\frac{\partial u_{Gj}}{\partial x_i}-\frac{\partial u_{Gi}}{\partial x_j}\right)\dot{x}_j+\left(\frac{\partial v_{Gj}}{\partial x_i}-\frac{\partial u_{Gi}}{\partial y_j}\right)\dot{y}_j\right]-\frac{1}{2}\frac{\partial}{\partial x_i}\sum_j[u_{Gj}^2+v_{Gj}^2+gh_j], \tag{4.17a}$$

$$+q_i\,\dot{x}_i=\sum_{j\neq i}\left[\left(\frac{\partial u_{Gj}}{\partial y_i}-\frac{\partial v_{Gi}}{\partial x_j}\right)\dot{x}_j+\left(\frac{\partial v_{Gj}}{\partial y_i}-\frac{\partial v_{Gi}}{\partial y_j}\right)\dot{y}_j\right]-\frac{1}{2}\frac{\partial}{\partial y_i}\sum_j[u_{Gj}^2+v_{Gj}^2+gh_j], \tag{4.17b}$$

$$q_i=\frac{\partial v_{Gi}}{\partial x_i}-\frac{\partial u_{Gi}}{\partial y_i}+f_i \tag{4.17c}$$

result from the requirement that $S(4.14)\,\mathrm{d}\tau$ be stationary with respect to $\delta\boldsymbol{x}_i(\tau)$ for all i. Unlike (3.8), the equations (4.17) for $\dot{\boldsymbol{x}}_i$ involve the velocities $\dot{\boldsymbol{x}}_j(j\neq i)$ of nearby fluid particles. This is a characteristic property of filtered models. For Rossby numbers of 0.01 and less (based on the lengthscale r_0 and the r.m.s. particle velocity) I have found that (4.17) can efficiently be solved for the $\dot{\boldsymbol{x}}_i$ by iterative adjustment of the left-hand sides. For higher Rossby numbers, other methods will have to be used. A sequel paper will report the application of a two-layer version of (4.17) to a model

Experiment	r_0	N_s	N	CPU time per step
I	1.6λ	80	792	3.8 s
II	0.8λ	65	2499	15.8 s

TABLE 1

of the ocean's main thermocline. Section 5 describes some solutions of the numerical equations of §3.

5. Numerical example

Griffiths, Killworth & Stern (1982) recently described a new type of parallel-flow instability for the same fluid system considered in this paper. They suppose that the initial blob is a narrow ribbon of fluid in near-geostrophic balance. If the ribbon width W is comparable to the Rossby deformation radius,

$$\lambda \equiv \frac{(gH)^{\frac{1}{2}}}{f} \tag{5.1}$$

(where H is the maximum fluid depth), then the ribbon develops varicose meanders. The meanders grow and the ribbon eventually breaks up into a chain of closed anticyclonic eddies. If the initial potential vorticity is uniform, then linear theory predicts that the meander wavelength for fastest growth is slightly larger than $2\pi\lambda$ and relatively insensitive to W for all $W \lesssim 2\lambda$. Laboratory experiments confirm these predictions.

In this section I describe two numerical experiments using the same assumptions and parameter settings as Griffiths *et al.* The initial blob is an annulus with width 2λ and radius 10λ (see table 1). The two experiments differ in the sampling radius r_0 and in the number of particles N_s in a sampling area πr_0^2 at time zero. These two factors determine N, the total number of particles.

The equations (3.8) were centre-stepped on a minicomputer. A time step of 0.01 rotation periods (0.01 RP) conserved the energy (3.9) to within one per cent over 1000 steps. The results (figures 2 and 3) closely resemble the laboratory photos of Griffiths *et al.* (1982). Both the experiments shown begin from the state of rest and reach geostrophic equilibrium within 2 RP. After 3–4 RP, meanders appear with the wavelength predicted by Griffiths *et al.* The meanders evolve into nearly isolated lumps within 6–9 RP. Experiment II has twice the resolution r_0^{-1} and about three times as many fluid particles as has experiment I. In experiment II, however, the number of fluid particles per sampling area is slightly less than in experiment I. The end states are qualitatively similar, but II evolves somewhat more slowly than I.

The depth estimator (3.1) forces the particle concentration to vanish at the blob boundaries, where the depth is zero. In consequence, the zero contours in figures 2 and 3 are poorly determined in a statistical sense. I believe that this is the most serious defect in the method as currently proposed. One remedy would allow particles near the blob edge to fission into more particles with smaller individual masses such that total mass, energy, etc. are conserved. Unfortunately, this idea involves *ad hoc* programming decisions. The experiments described here are preliminary, and mainly illustrate the practicality of the methods proposed.

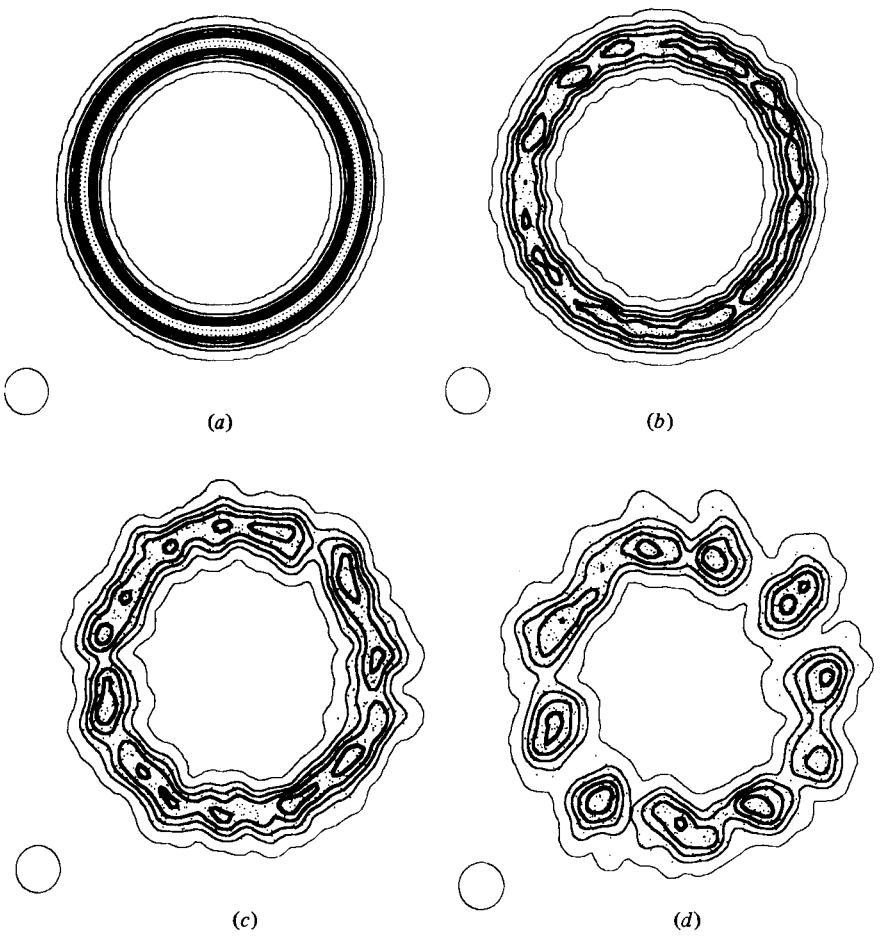

FIGURE 2. The fluid annulus in experiment 1 after (*a*) 0, (*b*) 2.0, (*c*) 3.6 and (*d*) 6.4 rotation periods. Darker contours correspond to greater fluid depth. The circles at lower left have radius r_0.

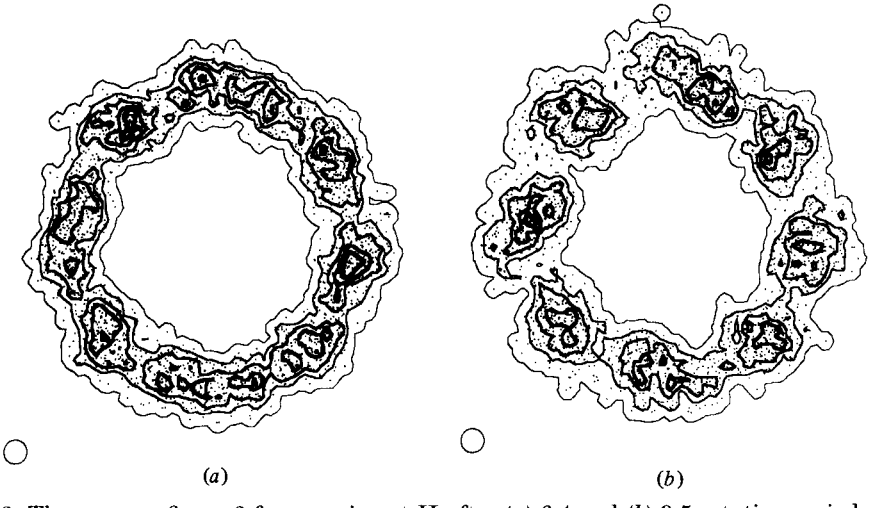

FIGURE 3. The same as figure 2 for experiment II after (*a*) 6.4 and (*b*) 9.5 rotation periods.

6. Discussion

The methods of this paper generalize easily to continuously stratified and multi-layered flows. Non-conservative forcing and damping can be included, but they must be inserted into the equations after the variational principle has been invoked. This is not a major defect in the method, because the non-conservative force laws are usually much simpler than pressure or inertia. Solid boundaries present no special difficulties, because the boundaries correspond to infinite potential walls. Since these potentials depend only on particle locations, they do not disturb the time and particle-label symmetries. Hence the conservation laws remain intact.

As previously remarked, the numerical equations of §§3 and 4 do not conserve analogues of the potential vorticity on particles, because the discretization destroys the symmetry property corresponding to infinitesimal variations in the particle labels. The conservation law would be preserved if a potential vorticity were assigned to each particle *a priori*, in the same way as mass. However, such assignment uses a consequence of the variational principle (potential-vorticity conservation) to modify the variational principle itself. This is legal only if the subsequently allowed variations conserve potential vorticity. One way to assure compliance would be to express the rotational velocity as a functional of the particle locations and the given (invariant) potential vorticity on particles. The irrotational velocity, which does not contribute to potential vorticity, would still be freely varied. Unfortunately, this procedure seems too complicated to be practical. Perhaps there is a simpler way.

The geostrophic model (4.4) was not – but could have been – obtained as the second step in a systematic iterative procedure. In this paper, specific methods and results are secondary to the general theme that conservation laws are important and are automatically maintained if the approximations bear on the Hamiltonian itself. Nonetheless, (4.4) is a significant result. McWilliams & Gent (1980) have recently reviewed and extended the general class of low-Rossby-number model equations which are intermediate in accuracy between the quasigeostrophic and primitive equations. However, none of the models discussed by McWilliams & Gent conserve analogues of both energy and potential vorticity in the general case of non-constant Coriolis parameter.

This work was supported by the National Science Foundation (OCE-8117696). I gratefully acknowledge numerous helpful discussions with Annalisa Griffa.

REFERENCES

AREF, H. & POMPHREY, N. 1981 Instability and chaotic motion of four vortices. *La Jolla Inst. Tech. Note* 81–133.

BROER, L. J. F. & KOBUSSEN, J. A. 1974 Conversion from material to local coordinates as a canonical transformation. *Appl. Sci. Res.* **29**, 419–429.

BUNEMAN, O. 1982 Advantages of Hamiltonian formulations in computer simulations. *Am. Inst. Phys. Proc.* **88**, 137–143.

CLEBSCH, A. 1859 Über die Integration der hydrodynamischen Gleichungen. *Crelles' J.* **56**, 1–10.

ECKART, C. 1960 Variation principles of hydrodynamics. *Phys. Fluids* **3**, 421–427.

GRIFFA, A. 1982 Canonical transformations and variational principles for fluid dynamics. (Unpublished manuscript.)

GRIFFITHS, R. W., KILLWORTH, P. D. & STERN, M. E. 1982 Ageostrophic instability of ocean currents. *J. Fluid Mech.* **117**, 343–377.

HARLOW, F. H. & WELCH, J. E. 1965 Numerical calculation of time-dependent viscous incompressible flow of fluid with a free surface. *Phys. Fluids* **8**, 2182–2189.

HERIVEL, J. W. 1955 The derivation of the equations of motion of an ideal fluid by Hamilton's principle. *Proc. Camb. Phil. Soc.* **51**, 344–349.

MCWILLIAMS, J. C. & GENT, P. R. 1980 Intermediate models of planetary circulations in the atmosphere and ocean. *J. Atmos. Sci.* **37**, 1657–1678.

RIPA, P. 1981 Symmetries and conservation laws for internal gravity waves. *Am. Inst. Phys. Proc.* **76**, 281–306.

SAARLOOS, W. VAN 1981 A canonical transformation relating the Lagrangian and Eulerian description of ideal hydrodynamics. *Physica* **108A**, 557–566.

SALMON, R. 1982*a* The shape of the main thermocline. *J. Phys. Oceanogr.* **12**, 1458–1479.

SALMON, R. 1982*b* Hamilton's principle and Ertel's theorem. *Am. Inst. Phys. Proc.* **88**, 127–135.

SELIGER, R. L. & WHITHAM, G. B. 1968 Variational principles in continuum mechanics. *Proc. R. Soc. Lond.* **A305**, 1–25.